Identification of Histidine 118 in the D1 Polypeptide of Photosystem II as the Axial Ligand to Chlorophyll Z[†]

David H. Stewart,[‡] Agnes Cua,[§] Dexter A. Chisholm,[||] Bruce A. Diner,[||] David F. Bocian,[§] and Gary W. Brudvig*,[‡]

Department of Chemistry, Yale University, New Haven, Connecticut 06520-8107, Department of Chemistry, University of California, Riverside, California 92521-0403, and Central Research and Development Department, Experimental Station, E. I. DuPont de Nemours and Company, Wilmington, Delaware 19880

Received March 23, 1998; Revised Manuscript Received May 13, 1998

ABSTRACT: Chlorophyll Z (Chl$_Z$) is a redox-active chlorophyll (Chl) which is photooxidized by low-temperature (<100 K) illumination of photosystem II (PSII) to form a cation radical, Chl$_Z^+$. This cofactor has been proposed to be an "accessory" Chl in the PSII reaction center and is expected to be buried in the transmembrane region of the PSII complex, but the location of Chl$_Z$ is unknown. A series of single-replacement site-directed mutants of PSII were made in which each of two potentially Chl-ligating histidines, D1-H118 or D2-H117, was substituted with amino acids which varied in their ability to coordinate Chl. Assays of the wild-type and mutant strains showed parallel phenotypes for the D1-118 and D2-117 mutants: noncoordinating or poorly coordinating residues at either position decreased photosynthetic competence and impaired assembly of PSII complexes. Only the mutants substituted with glutamine (D1-H118Q and D2-H117Q) had phenotypes comparable to the wild-type strain. The Chl$_Z^+$ cation was characterized by low-temperature electron paramagnetic resonance (EPR), near-infrared (IR) absorbance, and resonance Raman (RR) spectroscopies in wild-type, H118Q, and H117Q PSII core complexes. The quantum yield of Chl$_Z^+$ formation is the same (∼2.5% per saturating flash at 77 K) for wild-type, H118Q, and H117Q, indicating that its efficiency of photooxidation is unchanged by the mutations. Similarly, the EPR and near-IR absorbance spectra of Chl$_Z^+$ are insensitive to the mutations made at D1-118 and D2-117. In contrast, the RR signature of Chl$_Z^+$ in H118Q PSII, obtained by selective near-IR excitation into the Chl$_Z^+$ cation absorbance band, is significantly altered relative to wild-type PSII while the RR spectrum of Chl$_Z^+$ in the H117Q mutant remains identical to wild-type. Shifts in the RR spectrum of Chl$_Z^+$ in H118Q reflect a change in the structure of the Chl ring, most likely due to a perturbation of the core size and/or extent of doming caused by a change in the axial ligand to Mg(II). Thus, we conclude that the axial ligand to Chl$_Z$ is H118 of the D1 polypeptide. Furthermore, we propose that H117 of the D2 polypeptide is the ligand to a homologous redox-inactive accessory Chl which we term Chl$_D$. The Chl Z and D terminology reflects the 2-fold structural symmetry of PSII which is apparent in the redox-active tyrosines, Y$_Z$ and Y$_D$, and the active/inactive branch homology of the D1/D2 polypeptides with the L/M polypeptides of the bacterial reaction center.

Photosystem II (PSII)[1] is a membrane-bound protein complex which is responsible for photochemically catalyzing the oxidation of water to dioxygen. The assembly of polypeptides which comprise PSII contains a large array of chlorophyll (Chl) molecules that are used to collect light energy, transfer energy to the reaction center, and initiate photochemistry by inducing electron-transfer reactions. Most of the Chls found in PSII are bound to light-harvesting proteins and the Chl-binding proteins (CP43, CP47). The reaction center core contains only 5−7 Chls, which are isolated with the D1 and D2 polypeptides (1−6). By analogy to the bacterial photosynthetic reaction center (BRC), two of these Chls are thought to make up a "special-pair"-like dimer while two others are expected to be nearby monomeric "voyeur" Chls. The location of the remaining Chls is unknown, and analogy to the BRC is exhausted because the BRC contains only four bacteriochlorophylls (BChls). How-

[1] Abbreviations: BChl, bacteriochlorophyll; BRC, purple non-sulfur bacterial photosynthetic reaction center; Chl, chlorophyll; CP43/CP47, chlorophyll-binding proteins; cyt b_{559}, cytochrome b_{559}; D1/D2, core polypeptides of PSII; DCMU, 3-(3,4-dichlorophenyl)-1,1-dimethylurea; DM, n-dodecyl β-D-maltoside; EDTA, ethylenediaminetetraacetic acid; EPR, electron paramagnetic resonance; HEPES, N-(2-hydroxyethyl)-piperazine-N'-2-ethanesulfonic acid; IR, infrared; L/M, core polypeptides of the BRC; MES, 2-(N-morpholino)ethanesulfonic acid; PSI, photosystem I; PSII, photosystem II; Q$_A$/Q$_B$, electron-accepting quinones; RR, resonance Raman; SERDS, shifted-excitation Raman difference spectroscopy; Y$_D$/Y$_Z$, redox-active tyrosines.

ever, there are two histidines present in the D1/D2 sequence (D1-H118 and D2-H117) which do not have homologues in the L/M subunits of the BRC (7). Interestingly, these are the only two histidines in the transmembrane region of PSII that are not assigned as ligands to known cofactors. Because histidine is a common axial ligand to Chl, these are likely ligands for two of the reaction center Chls.

It has been speculated by a number of groups that the histidines at positions D1-118 and D2-117 are ligands to "accessory" Chls (8–12), and site-directed mutations at D1-H118 in *Chlamydomonas reinhardtii* are consistent with this assignment (13). Fluorescence energy-transfer measurements give a distance between P680 and an accessory Chl of 30 Å; this distance is similar to that measured between the special pair and the residue which corresponds to H118 in the BRC, L-C92 (9). These residues have also been suggested as possible ligands to the redox-active Chl known as chlorophyll Z (Chl$_Z$) based on the measured distance between Chl$_Z^+$ and the non-heme Fe(II) in PSII (39.5 ± 2.5 Å) and the calculated distance between the non-heme Fe(II) and the H118/H117 homologues in the BRC, L-C92 ($\sim$36 Å) and M-F119 ($\sim$39 Å) (12). The location and identity of Chl$_Z$ are of particular interest because Chl$_Z$ is an intermediate in the electron-transfer pathway between cytochrome b_{559} (cyt b_{559}) and P680$^+$ (14). Chl$_Z$ is expected to be in close proximity to the heme of cyt b_{559} because the oxidation of cyt b_{559} by Chl$_Z$ is very efficient, even at cryogenic temperatures (14, 15). Although the rates and yields of photooxidation of cyt b_{559} and Chl$_Z$ are low relative to the primary electron donors (Y$_Z$ and the oxygen-evolving complex), these "alternate" electron donors can mediate cyclic electron transfer and may have a role in protection of PSII from photoinactivation (14, 16–20). Consistent with this idea, it has been shown that the Chl$_Z^+$ cation is a potent quencher of fluorescence in PSII (21).

A recent advance in the application of resonance Raman (RR) spectroscopy has led to a technique, shifted-excitation Raman difference spectroscopy (SERDS) (22, 23), which effectively eliminates fluorescence interference from Raman scattering so that RR spectra can be collected for highly fluorescent proteins such as photosystem II. SERDS has been utilized to obtain detailed structural, vibrational, and electronic information about BChls and bacteriopheophytins in the BRC (24–27). So far, SERDS has not been used to study specific Chls in the PSII complex because of the spectral overlap of the Chl Q$_Y$ absorbance bands. The near-infrared (IR) absorbance bands associated with Chl cations ($\sim$800–850 nm) provide a way to circumvent this limitation. The Chl cation absorbance bands, which are isolated from the absorbance bands of the neutral Chls, can be excited selectively by near-IR irradiation to generate RR spectra of the cations, isolated from the large background of neutral Chls (28).

We have exploited these characteristics to study Chl$_Z^+$, which can be trapped quantitatively by low-temperature illumination of PSII. Until now, Chl$_Z$ has been a phenomenological entity with a characteristic electron paramagnetic resonance (EPR) signal and known conditions required to generate this signal, but an uncertain identity. In this paper, we provide direct experimental evidence that D1-H118 is the axial ligand to an accessory Chl and that this accessory Chl is the redox-active chlorophyll, Chl$_Z$. Furthermore, we

show that D2-H117 is a likely ligand to an accessory Chl, a redox-inactive Chl which we term Chl$_D$.

MATERIALS AND METHODS

Strains and Construction of Mutants. Mutations were introduced into a glucose-tolerant strain of *Synechocystis* PCC 6803 (29). Mutagenesis of the psbD1 gene (encoding the D2 protein) was performed as described in Tang et al. (30). Mutagenesis of the psbA3 gene (encoding the D1 protein) was performed as described in Nixon et al. (31). In both cases, the Stratagene QuickChange system was used to generate mutant constructs. Mutations were confirmed by sequencing PCR products amplified from fully segregated *Synechocystis* mutants.

In this work, wild-type *Synechocystis* refers to a strain containing all three copies of the psbA gene and both copies of the psbD gene. PSII isolated from *Synechocystis* strains containing wild-type copies of only psbA3 (TC31) or psbD1 would be the true controls for the D1 and D2 mutants, respectively. However, TC31 displays identical absorbance properties and electron-transfer kinetics compared to wild-type *Synechocystis* (31, B. A. Diner, unpublished results), and we find that the properties of Chl$_Z$ in the wild-type and psbD1-only strains are identical (see below). Therefore, we used PSII isolated from wild-type *Synechocystis* as the control for the site-directed mutants.

Preparation of PSII Core Complexes. Cells of *Synechocystis* were grown photoheterotrophically at 30 °C in 18 L carboys containing BG-11 medium (32) supplemented with 5 mM glucose and bubbled with 5% CO$_2$ in air. O$_2$-evolving PSII core complexes were isolated from these cells using the procedure of Tang and Diner (33). Both O$_2$-evolution assays and sodium dodecylsulfate–polyacrylamide gel electrophoresis indicated low levels (<10%) of photosystem I (PSI) contamination. To simplify the PSII complexes, they were depleted of the Mn$_4$ cluster by treatment with 5 mM NH$_2$OH and 5 mM EDTA in Chenaie's buffer A (50 mM MES, pH 6.5, 15 mM NaCl, 1 mM CaCl$_2$, 0.4 M sucrose) plus 0.03% *n*-dodecyl β-D-maltoside (DM) followed by washing with 5 mM EDTA in buffer A to remove unbound Mn(II) (34). The PSII core complexes were stored in 50 mM MES, pH 6.0, 20 mM CaCl$_2$, 10 mM NaCl, 20% (v/v) glycerol, and 0.03% DM at 77 K in the dark until further use. Determinations of Chl concentration were made by extraction into methanol and using $\epsilon_{665} = 79.24$ mL (mg of Chl)$^{-1}$ cm^{-1} for Chl *a* in methanol (35).

Quantitation of PSII in Whole Cells. The PSII content was quantitated relative to wild-type for mutant *Synechocystis* cells by monitoring the magnitude of the variable fluorescence arising from the photoreduction of Q$_A$ in a series of 20 xenon flashes at room temperature. Cells suspended in BG-11 medium plus glucose (OD$_{730}$ = 0.9), supplemented with 50 mM HEPES, pH 7.5, were made 0.3 mM in 1,4-benzoquinone and 0.3 mM in K$_3$Fe(CN)$_6$ and incubated for at least 10 min in the dark. The suspension was made 40 μM in DCMU, and the variable fluorescence was measured within 30 s of the addition of 20 mM NH$_2$OH.

EPR Spectroscopy. Cryogenic EPR spectra were collected on a Varian E-line EPR spectrometer equipped with an Oxford Instruments ESR 900 liquid helium cryostat. The spectrometer conditions were the following: microwave

frequency, 9.28 GHz; microwave power, 0.05 mW; magnetic field modulation amplitude, 4 G; temperature, 30 K. These are nonsaturating conditions for the Chl_Z^+ EPR signal. The quantum yield of photooxidation of Chl_Z^+ at 77 K was measured by EPR after single, saturating laser flashes delivered by a flash-lamp pumped Candela SLL-66A dye laser containing rhodamine chloride 590 in a 50:50 methanol/water solution. The flashes were focused onto the sample in the EPR tube with a cylindrical planoconvex lens while the EPR tube was immersed in a quartz finger Dewar containing liquid nitrogen. Because the Chl_Z^+ signal decays about 10% in 10 min at 77 K, it was important to return the sample to the EPR cavity (at 30 K) immediately after each flash was performed. Chl_Z^+ decays less than 4% over 10 min at 30 K. After 10 or more flashes, the full yield of photooxidized Chl_Z^+ was generated by continuous illumination of the sample at 77 K for 10 min with a 100 W quartz/halogen lamp. The PSII samples were at a concentration of 0.43 mg of Chl/mL in 50 mM MES, pH 6.0, 20 mM $CaCl_2$, 10 mM NaCl, 40% (v/v) glycerol and were treated with 40–75 μM $K_3Fe(CN)_6$ to oxidize cyt b_{559}. Prior to illumination, the samples were dark-adapted for 2–3 h at 0 °C to allow oxidized Y_D to decay completely.

Optical Spectroscopy. Optical spectra of the near-IR cation absorbance band of Chl_Z^+ were collected using a Perkin-Elmer Lambda 6 UV/Vis spectrophotometer. The measurements were made at 77 K by using a home-built Plexiglas flat cell (path length ~1/32 in.) immersed in liquid nitrogen in a quartz finger Dewar. Condensation buildup on the quartz surface was prevented by a flow of dry N_2 gas. Interference due to bubbling of the liquid nitrogen was eliminated by careful cleaning of the quartz surface with a basic ethanol solution (0.125 g of KOH/mL). The optical samples were frozen as uncracked glasses by slow immersion into a liquid nitrogen bath. Both nonilluminated and illuminated spectra were collected; illumination consisted of 15 min of continuous white light at 77 K as described above. The PSII samples were at a concentration of ~3 mg of Chl/mL in 50 mM MES, pH 6.0, 20 mM $CaCl_2$, 10 mM NaCl, 40% (v/v) glycerol and were treated with 1 mM K_2IrCl_6 and 0.1 mM $K_3Fe(CN)_6$ to oxidize cyt b_{559}.

RR Spectroscopy. The RR measurements were made at cryogenic temperatures (30–50 K) on highly concentrated, glassy samples contained in 1 mm i.d. capillary tubes. The sampling accessories, spectrometer, and laser systems have been previously described (*36, 37*). Each RR data set was obtained with 2 h of signal averaging. Cosmic spikes in the individual scans were removed prior to coaddition of the scans. The spectral resolution was ~2 cm^{-1}. The laser power was ~5 mW. The spectral data were calibrated using the known frequencies of fenchone. Both nonilluminated and illuminated spectra were collected; illumination consisted of 15 min of continuous white light from a focused 200 W quartz/halogen lamp at low temperature (30–50 K). The PSII samples were at a concentration of 6–12 mg of Chl/mL in 50 mM MES, pH 6.0, 20 mM $CaCl_2$, 10 mM NaCl, 40% (v/v) glycerol and were treated with 250 μM $K_3Fe(CN)_6$ to oxidize cyt b_{559}.

All of the RR spectra were acquired using the SERDS technique in order to reduce the level of interference from fluorescence (*22, 23*). The application of the SERDS method to photosynthetic proteins has been previously described in

Table 1: Summary of D1-H118 and D2-H117 Mutants Made, Their Photosynthetic Competence, and the Level of PSII Assembly Relative to Wild-Type

residue introduced	photosynthetic growth		PSII level (%) relative to WT	
	H118 (D1)	H117 (D2)	H118 (D1)	H117 (D2)
glutamine (Q)	+++	+++	100	100
lysine (K)	+	+	10	12
glutamate (E)	−	−	≤10	10
aspartate (D)	−	ND^a	15	ND
alanine (A)	−	ND	15−20	ND
glycine (G)	−	ND	low	ND
leucine (L)	−	ND	low	ND

^{a} ND = not determined.

detail (*22−27*). Briefly, each data set is acquired at two excitation wavelengths that differ by a small wavenumber increment (typically 10 cm^{-1}). [The 2 h data acquisition time indicated above is for each of the two data sets required to construct a SERDS trace.] These data sets are subtracted to yield a background-free RR difference (SERDS) spectrum. The RR data presented herein were obtained by subtracting the initial spectrum from the shifted spectrum. The spectral window is defined by the initial spectrum and corresponds to the wavenumber axis in the figures. The normal RR spectrum is then reconstructed from the SERDS data by fitting the latter to a series of derivative-shaped functions (in this case, difference bands generated from Gaussian functions) of arbitrary frequency, amplitude, and width. The frequencies marked in the figures correspond to the positions of the bands used in the fits and thus do not necessarily correspond to the peak maxima for overlapping bands. In addition, certain bands are marked that are not clearly resolved in the spectra. These bands are indicated because their inclusion noticeably improved the quality of the fits to the SERDS data based on the residuals (observed spectra minus fits).

RESULTS AND DISCUSSION

Site-Directed Mutants and Cell Growth Properties. To probe the proposed accessory Chl/Chl_Z binding sites, a series of single-replacement substitutions were made at the D1-H118 and D2-H117 positions. The site-directed mutants made are summarized in Table 1 along with a rating of their photosynthetic competence and the extent to which they assembled PSII. The amino acids substituted for histidine vary in their expected ability to coordinate Chl, ranging from likely axial ligands (glutamine) to noncoordinating residues (glycine). A comparison of the phenotypes shows that both photosynthetic competence and the ability to assemble PSII complexes closely correspond to the ability of the substituted residue to serve as a ligand to Chl. In the case of noncoordinating amino acids, the mutant strains are non-photosynthetic and assemble ≤20% of the wild-type level of PSII complexes. Substitutions of possibly coordinating residues such as lysine, glutamate, and aspartate are significantly impaired in their ability to do photosynthesis and only produce about 10% of the level of PSII centers per cell when grown photoheterotrophically. The glutamine mutants, which are expected to coordinate Chl, are unimpaired relative to wild-type. An important observation from these comparisons is the parallel behavior of the D1-118 and D2-117
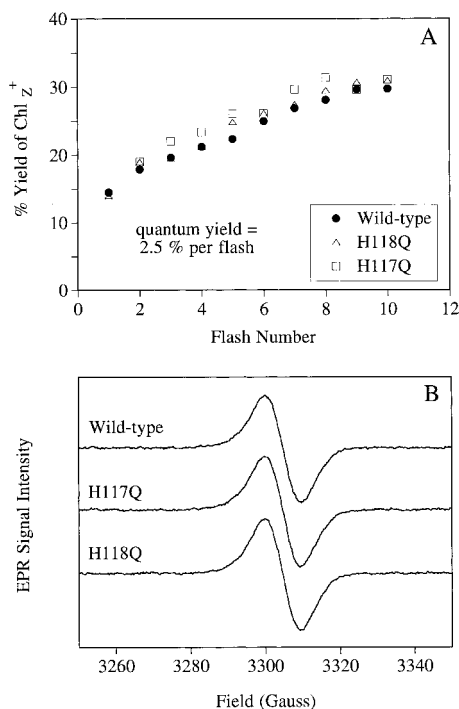
FIGURE 1: (A) The quantum yield of Chl$_Z^+$ photooxidation measured by EPR after single, saturating laser flashes at 77 K. The full yield of Chl$_Z^+$ was obtained by continuous illumination for 10 min at 77 K. (B) Illuminated minus nonilluminated EPR spectra of Chl$_Z^+$ in wild-type, H117Q, and H118Q PSII core complexes. The spectra are vertically shifted for clarity.

mutants across the range of amino acid substitutions. The strong dependence of photosynthetic prowess and PSII levels on the coordinating ability of the histidine substitute at both the D1-118 and D2-117 sites suggests that D1-H118 and D2-H117 are both ligands to accessory Chls. It is expected that impairment of Chl binding in the PSII reaction center will have a direct effect on the development of the photosynthetic apparati in growing cells. This phenomenon has been observed previously in *Synechocystis* (*38*). Replacement of histidine with glutamine has been shown to be a conservative mutation that maintains function and that potentially provides a spectroscopic signature for its replacement (B. A. Diner, in preparation). Because of the photosynthetic competence of the D1-H118Q and D2-H117Q strains and levels of PSII centers comparable to wild-type, we chose to focus on these mutants for spectroscopic studies to determine whether D1-H118 and/or D2-H117 is a ligand to Chl$_Z^+$.

Quantum Yield of Chl$_Z^+$ Formation. Initially it was important to show that Chl$_Z^+$ is generated by low-temperature photooxidation in the mutants, as is known to occur in wild-type PSII. The formation of Chl$_Z^+$ was characterized by monitoring the yield of the Chl$_Z^+$ EPR signal after saturating laser flashes at 77 K. The quantum yield is fairly constant over the first five flashes and has the same value within error (2.5% ± 0.3%) for wild-type, H117Q, and H118Q PSII (Figure 1A). The yield of Chl$_Z^+$ following each flash was normalized to the full yield of Chl$_Z^+$ produced by 10 min of continuous illumination at 77 K. A comparison of the Chl$_Z^+$ EPR signals for wild-type, H117Q, and H118Q PSII is presented in Figure 1B. It is clear from the two panels of Figure 1 that H117Q and H118Q are very similar to wild-type in both the efficiency with which Chl$_Z$ is photooxidized and the EPR properties of Chl$_Z^+$. The latter observation is
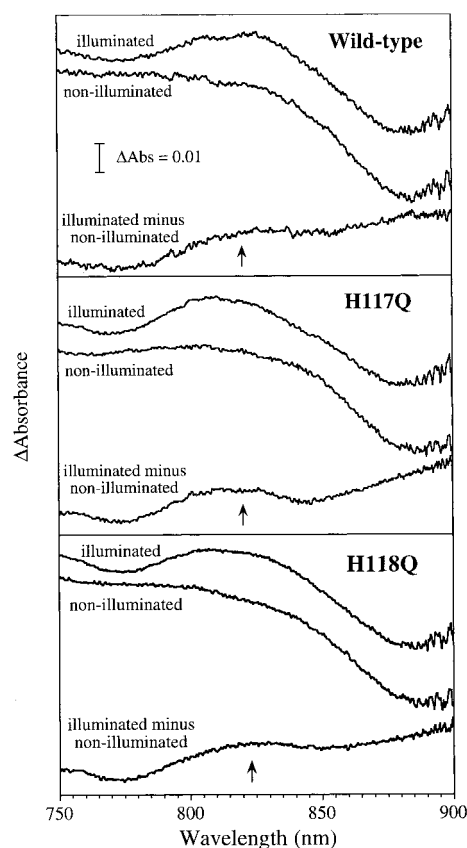

FIGURE 2: Illuminated, nonilluminated, and illuminated minus nonilluminated (Chl$_Z^+$) near-IR absorbance spectra of wild-type (top), H117Q (middle), and H118Q (bottom) PSII core complexes collected at 77 K. The excitation wavelengths used for the RR experiments are indicated with arrows.

expected because Chl cation EPR signals are typically isotropic and featureless, owing to delocalization of the unpaired electron over the tetrapyrrole macrocycle. Thus, the two glutamine mutants provide ideal systems for studying the effect on Chl$_Z$ of changing the accessory Chl ligands at D1-118 and D2-117.

Optical and RR Characterization of Chl$_Z^+$. The near-IR absorbance band which is found at ~800–850 nm for Chl cations provides a selective spectroscopic handle for studying Chl$_Z^+$ in the absence of interfering background absorbance from the excess of neutral Chls (~40) found in PSII core complexes. Figure 2 shows the absorbance spectra for Chl$_Z^+$ in wild-type, H117Q, and H118Q PSII. The cation band represents a weak electronic transition; as a result, fairly high sample concentrations are required to resolve the signal. In addition, the absorbance is very broad, making it difficult to determine a precise λ_{max} for each of the three samples. However, the Chl$_Z^+$ absorbance band for wild-type, H117Q, and H118Q appears to maximize in the 815–825 nm range. These signals represent an electronic transition that can be excited directly to generate RR spectra of Chl$_Z^+$ as we have previously shown in preliminary studies of the wild-type PSII core complex (*28*).

Near-IR excitation RR spectra of the PSII core complex are shown in Figures 3–6. Figure 3 compares the high-frequency raw (unsmoothed) SERDS traces obtained for illuminated versus nonilluminated samples of wild-type (top), H117Q (middle), and H118Q (bottom). The data acquisition conditions were as follows: wild-type, $\lambda_{ex} = 820$ nm and
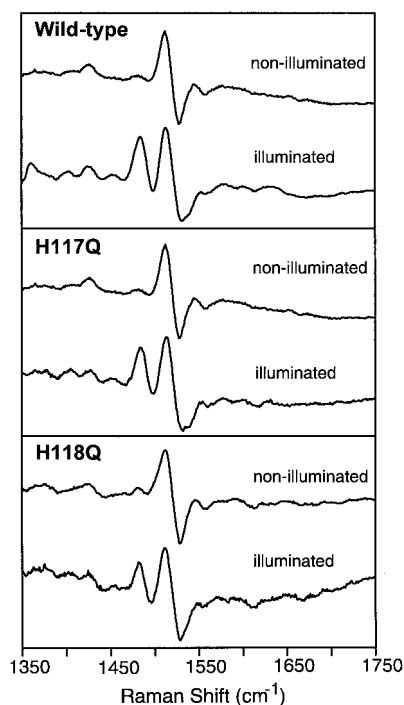
FIGURE 3: High-frequency near-IR-excitation SERDS data obtained for illuminated versus nonilluminated samples of wild-type (top), H117Q (middle), and H118Q (bottom) PSII core complexes. The data acquisition conditions were as follows: wild-type, $\lambda_{ex} = 820$ nm and 30 K; H117Q, $\lambda_{ex} = 820$ nm and 50 K; H118Q, $\lambda_{ex} = 823$ nm and 50 K.
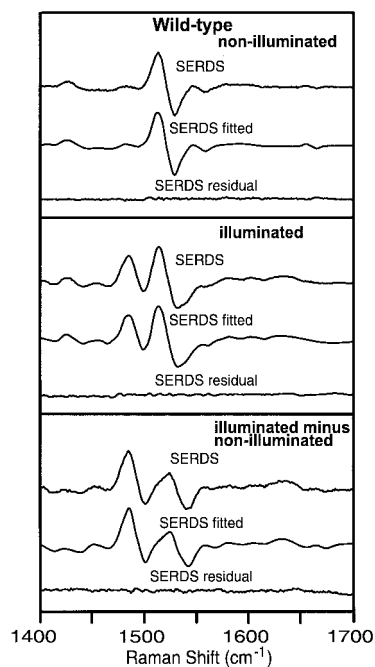

FIGURE 4: High-frequency near-IR-excitation SERDS data and fits for wild-type PSII core complexes. The three panels show the raw (unsmoothed) SERDS data, the fits of the SERDS data, and the SERDS residuals (observed minus fit) for nonilluminated (top panel), illuminated (middle panel), and illuminated minus nonilluminated (bottom panel) PSII core complexes. The data acquisition conditions were as in Figure 3.

30 K; H117Q, $\lambda_{ex} = 820$ nm and 50 K; H118Q, $\lambda_{ex} = 823$ nm and 50 K. Data were also acquired at other excitation wavelengths and temperatures (not shown); however, these data did not reveal any additional features.[2] Figure 4 shows the SERDS data analysis for wild-type. The three panels
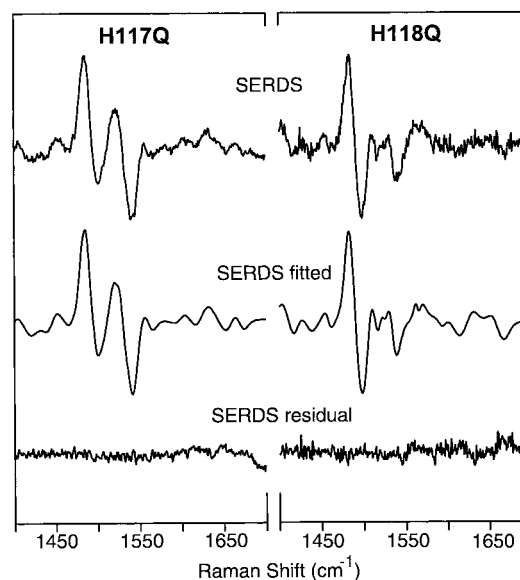

FIGURE 5: Near-IR-excitation SERDS spectra of $Chl_Z{}^+$ (illuminated minus nonilluminated difference spectra) in H117Q (left panel) and H118Q (right panel) PSII core complexes. In each panel, the top trace is the raw difference SERDS data, the middle trace is the fit of the difference SERDS data, and the bottom trace is the SERDS residual (observed minus fit). The data acquisition conditions were as in Figure 3.
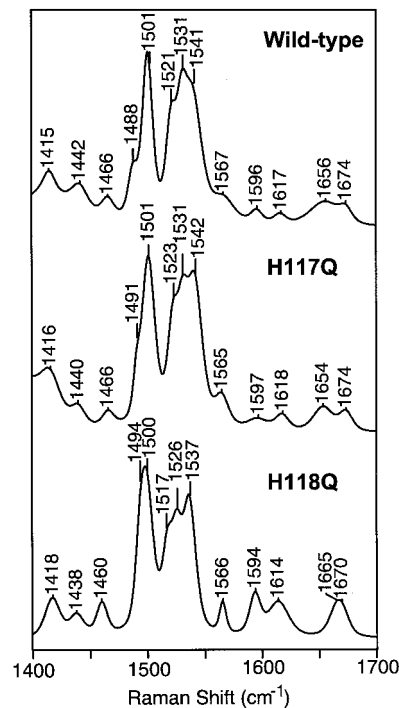

FIGURE 6: Comparison of the near-IR-excitation RR spectra of $Chl_Z{}^+$ reconstructed from the SERDS data from wild-type (top), H117Q (middle), and H118Q (bottom) PSII core complexes. The data acquisition conditions were as in Figure 3.

show the raw (unsmoothed) SERDS data, the fits of the SERDS data, and the SERDS residuals (observed minus fit) for nonilluminated (top panel), illuminated (middle panel), and illuminated minus nonilluminated (bottom panel) PSII. Figure 5 shows the salient difference SERDS data sets for H117Q (left panel) and H118Q (right panel). The top traces are the raw (unsmoothed) difference SERDS data (illuminated minus nonilluminated). The middle trace in each panel is the fit of the difference SERDS data, and the bottom

trace is the SERDS residual (observed minus fit). The relatively small residuals compared with the SERDS intensities in both Figures 4 and 5 are indicative of the excellent fidelity of the fits for all three PSII samples. To facilitate comparison, Figure 6 shows the RR spectra of Chl$_Z^+$ reconstructed from the difference SERDS data (illuminated minus nonilluminated) from wild-type PSII and the two mutants.

Inspection of Figure 3 reveals that the illumination-induced spectral changes observed for the two mutants are qualitatively similar to one another and similar to those observed for wild-type PSII. These changes include the appearance of a number of new signals that gain intensity (relative to the features present prior to illumination) as the excitation wavelength is tuned from the blue side of the near-IR absorbance band of Chl$_Z^+$, maximize with excitation in the 820−825 nm region, and lose intensity with excitation on the red side of the cation band (see also *28*). However, closer inspection of illumination-induced spectral features reveals the following important differences between the characteristics of H118Q and H117Q. First, the positions of certain spectral features of the former mutant are shifted relative to those of wild-type, whereas the spectrum of the latter mutant is to within experimental error the same as that of wild-type. This effect is apparent even in the unprocessed SERDS data (Figure 3), but is more readily seen in the reconstructed spectra (Figure 6). For example, Chl$_Z^+$ in both H117Q and wild-type exhibits a group of strong RR bands at ∼1541, ∼1531, and ∼1523 cm^{-1}. The analogous bands of H118Q are downshifted to ∼1536, ∼1526, and ∼1517 cm^{-1}. Second, the maximum intensities for the RR bands of Chl$_Z^+$ in both H117Q and wild-type are observed with λ_{ex} ∼820 nm. The maximum RR intensities for H118Q are observed with excitation slightly to the red with λ_{ex} ∼823 nm. Collectively, the RR scattering characteristics observed for Chl$_Z^+$ in the wild-type and the two mutant PSII complexes are most consistent with the view that the cation radical is formed only on the Chl cofactor in the D1 polypeptide and that residue D1-H118 (or D1-Q118) serves as the axial ligand to the Mg(II) ion of this cofactor.

The vibrational frequencies of the ring-skeletal modes of Chl are sensitive to changes in the conformation of the macrocycle and the number and nature of the axial ligands (*39*). The salient observation of the present study is that the frequencies of certain ring-skeletal modes of Chl$_Z^+$ in H118Q PSII are clearly shifted relative to the analogous modes of wild-type, whereas these shifts are not observed for Chl$_Z^+$ in H117Q PSII.[3] The shifts in the ring-skeletal modes are consistent with a change in the core size and/or extent of doming of the Chl macrocycle. These shifts most likely reflect a perturbation of the Chl$_Z$ conformation caused by a change in the axial ligand of Chl$_Z$ from histidine to glutamine. On the other hand, it is also plausible that

conformational changes could be induced in Chl$_Z$ by nonspecific interactions with the D1-118 residue if this residue is in close proximity to the cofactor, but does not serve as an axial ligand. We do not favor this interpretation for two reasons (*40*). First, the modes that exhibit shifts are known to be sensitive to changes in axial ligation. Second, the magnitude of the shifts (∼5 cm^{-1}) is consistent with that expected for a change in the type of axial ligand while maintaining the coordination number the same (pentacoordinate). Therefore, we conclude that H118 of the D1 polypeptide is the axial ligand to the redox-active accessory Chl, Chl$_Z$. In addition, we suggest that D2-H117 is the axial ligand to a redox-inactive Chl which is the homologue of Chl$_Z$ on the D2 polypeptide. We propose that this redox-inactive accessory Chl be called Chl$_D$.

CONCLUSIONS

In this paper, we have identified D1-H118 and D2-H117 as ligands to accessory Chls in the reaction center of PSII. We have utilized RR with near-IR excitation of the Chl$_Z^+$ cation band to probe selectively the structure of Chl$_Z^+$. D1-H118 has been identified as the axial ligand to the redox-active Chl$_Z$, and D2-H117 is proposed to be the axial ligand to a redox-inactive accessory Chl which we call Chl$_D$. The Chl Z and D terminology reflects the 2-fold structural symmetry of PSII which is observed for the redox-active tyrosines, Y$_Z$ and Y$_D$ (*41*), and is expected based on analogy to the BRC. The present study shows that this symmetry extends to the B helices of the D1/D2 polypeptides, at least in the case of the accessory Chls. Furthermore, this work is consistent with the description of the D1 and D2 polypeptides of PSII as active and inactive branches, respectively, based on the distribution of redox-active components and analogy to the BRC (*42*). Finally, the identification of Chl$_Z$ as an accessory Chl ligated by D1-H118 disproves the idea that Chl$_Z$ is a kinetically stable form of the P680 chlorophyll cation.

The use of near-IR irradiation to study selectively the RR properties of Chl cations by excitation of the cation absorbance band has several obvious applications. Two other Chl

---

[2] The RR data acquired for the PSII samples in the 30−50 K range revealed that the RR cross sections for Chl$_Z^+$ in all three PSII complexes are strongly temperature dependent; the temperature dependence for the two mutants is similar, but different from that of wild-type. In particular, the RR cross section for Chl$_Z^+$ in the mutants is larger at 50 K than at 30 K, whereas the opposite is the case for wild-type. The origin of this difference is not clear and is currently under investigation. The spectra shown in the figures were obtained under conditions at which the RR intensities for Chl$_Z^+$ are approximately the same (relative to that of the neutral Chls) for all three PSII samples.

[3] The RR spectra exhibit bands in the 1650−1675 cm^{-1} region that are also sensitive to the H118Q mutation. These bands could be due to carbonyl stretching modes of the C$_9$-keto group. If these bands are indeed carbonyl stretches, the frequencies indicate that the C$_9$-keto group is very strongly hydrogen bound. In particular, the frequency of the C$_9$-keto stretch of a neutral Chl that is free of hydrogen bonding is typically near 1690 cm^{-1} (*39*). Oxidation to the cation radical *upshifts* the C$_9$-keto stretch by ∼25 cm^{-1} whereas hydrogen bonding (to either a neutral or a cation radical) downshifts this mode. The magnitude of the downshift depends on the strength of the hydrogen bond; however, the shifts are generally less than 40 cm^{-1} (*39*). Thus, C$_9$-keto stretches of a cation radical in the 1650−1675-cm^{-1} region would be downshifted 40−65 cm^{-1}, indicating unprecedented strong hydrogen-bonding interactions. For this reason, we suggest that the RR bands of Chl$_Z^+$ in the 1650−1675 cm^{-1} region are not carbonyl stretches, but instead are nonfundamental vibrations (combinations or overtones). In this regard, previous RR studies of BChl have shown that a number of nonfundamental modes are observed in this spectral region (*37*). Finally, we note that the RR bands observed in the 1650−1675 cm^{-1} region in the difference SERDS data set cannot be due to vibrations of neutral Chl because the frequencies are different from those observed for the nonilluminated samples. For example, fits of the SERDS data for nonilluminated wild-type PSII indicate that the neutral Chls exhibit bands at 1641 and 1662 cm^{-1}, whereas Chl$_Z^+$ exhibits bands at 1656 and 1674 cm^{-1}.

cations are formed during the initial steps of photosynthetic electron transfer, P700$^+$ of PSI and P680$^+$ of PSII. Neither of these species has been characterized by RR due to their spectral overlap with surrounding Chls. By combining the SERDS technique with selective cation excitation, important structural information about each of these Chls may be obtained. RR studies of the P700$^+$ cation, which is asymmetrically distributed over a Chl dimer (*43*), would provide structural information about this species and insight based on existing work on the BChl dimer, P, in the BRC. Of possibly greater significance, the location and identity of the P680$^+$ cation might be elucidated by RR studies of the Chl cation which is formed transiently during the initial charge separation in PSII. A study of the RR properties of the P680$^+$ cation, in mutants in which the potential ligands of the cation have been altered, might lead to identification of the P680$^+$ cation ligand, as was the case in this study. Based on analogy to the BRC, D1-H198 and D2-H197 are expected to ligate a "special pair"-like Chl dimer which may be the site of P680$^+$. Alternatively, there is evidence that the P680$^+$ cation resides on a Chl monomer (*44*), which could correspond to one of the "voyeur" BChls in the BRC. Since the positions in the CD helices of PSII which correspond to the "voyeur" BChl ligands in the BRC are noncoordinating residues, potential ligands to a P680$^+$ monomer might occupy nearby positions in the CD helix, such as D1-Q187 or D2-Q186.

REFERENCES

1. Nanba, O., and Satoh, K. (1987) *Proc. Natl. Acad. Sci. U.S.A. 84*, 109−112.
2. Gounaris, K., Chapman, D. J., Booth, P. J., Crystall, B., Giorgi, L. B., Klug, D. R., Porter, G., and Barber, J. (1990) *FEBS Lett. 265*, 88−92.
3. Kobayashi, M., Maeda, H., Watanabe, T., Nakane, H., and Satoh, K. (1990) *FEBS Lett. 260*, 138−140.
4. Montoya, G., Yruela, I., and Picorel, R. (1991) *FEBS Lett. 283*, 255−258.
5. Oren-Shamir, M., Sai, P. S. M., Edelman, M., and Scherz, A. (1995) *Biochemistry 34*, 5523−5526.
6. Setlíková, E., Ritter, S., Hienerwadel, R., Kopecky, J., Komenda, J., Welte, W., and Setlík, I. (1995) *Photosynth. Res. 43*, 201−211.
7. Michel, H., and Deisenhofer, J. (1988) *Biochemistry 27*, 1−7.
8. Vacha, F., Joseph, D. M., Durrant, J. R., Telfer, A., Klug, D. R., Porter, G., and Barber, J. (1995) *Proc. Natl. Acad. Sci. U.S.A. 92*, 2929−2933.
9. Schelvis, J. P. M., van Noort, P. I., Aartsma, T. J., and van Gorkom, H. J. (1994) *Biochim. Biophys. Acta 1184*, 242−250.
10. Ruffle, S. V., Donnelly, D., Blundell, T. L., and Nugent, J. H. A. (1992) *Photosynth. Res. 34*, 287−300.
11. Mulkidjanian, A. Y., Cherepanov, D. A., Haumann, M., and Junge, W. (1996) *Biochemistry 35*, 3093−3107.
12. Koulougliotis, D., Innes, J. B., and Brudvig, G. W. (1994) *Biochemistry 33*, 11814−11822.
13. Hutchinson, R. S., and Sayre, R. T. (1995) in *Photosynthesis: from Light to Biosphere* (Mathis, P., Ed.) pp 471−474, Kluwer Academic Publishers, Dordrecht.
14. Thompson, L. K., and Brudvig, G. W. (1988) *Biochemistry 27*, 6653−6658.
15. de Paula, J. C., Innes, J. B., and Brudvig, G. W. (1985) *Biochemistry 24*, 8114−8120.
16. Allakhverdiev, S. I., Klimov, V. V., and Carpentier, R. (1997) *Biochemistry 36*, 4149−4154.
17. Barber, J., and De Las Rivas, J. (1993) *Proc. Natl. Acad. Sci. U.S.A. 90*, 10942−10946.
18. Nedbal, L., Samson, G., and Whitmarsh, J. (1992) *Proc. Natl. Acad. Sci. U.S.A. 89*, 7929−7933.
19. Buser, C. A., Diner, B. A., and Brudvig, G. W. (1992) *Biochemistry 31*, 11449−11459.
20. Poulson, M., Samson, G., and Whitmarsh, J. (1995) *Biochemistry 34*, 10932−10938.
21. Schweitzer, R. H., and Brudvig, G. W. (1997) *Biochemistry 36*, 11351−11359.
22. Shreve, A. P., Cherepy, N. J., Franzen, S., Boxer, S. G., and Mathies, R. A. (1991) *Proc. Natl. Acad. Sci. U.S.A. 88*, 11207−11211.
23. Shreve, A. P., Cherepy, N. J., and Mathies, R. A. (1992) *Appl. Spectrosc. 46*, 707−711.
24. Czarnecki, K., Diers, J. R., Chynwat, V., Erickson, J. P., Frank, H. A., and Bocian, D. F. (1997) *J. Am. Chem. Soc. 119*, 415−426.
25. Cherepy, N. J., Shreve, A. P., Moore, L. J., Franzen, S., Boxer, S. G., and Mathies, R. A. (1994) *J. Phys. Chem. 98*, 6023−6029.
26. Cherepy, N. J., Shreve, A. P., Moore, L. J., Boxer, S. G., and Mathies, R. A. (1997) *J. Phys. Chem. 101*, 3250−3260.
27. Palaniappan, V., Schenck, C. C., and Bocian, D. F. (1995) *J. Phys. Chem. 99*, 17049−17058.
28. Cua, A., Stewart, D. H., Brudvig, G. W., and Bocian, D. F. (1998) *J. Am. Chem. Soc. 120*, 4532−4533.
29. Williams, J. G. K. (1988) *Methods Enzymol. 167*, 766−778.
30. Tang, X.-S., Chisholm, D. A., Dismukes, G. C., Brudvig, G. W., and Diner, B. A. (1993) *Biochemistry 32*, 13742−13748.
31. Nixon, P. J., Trost, J. T., and Diner, B. A. (1992) *Biochemistry 31*, 10859−10871.
32. Rippka, R., Deruelles, J., Waterbury, J. B., Herdman, M., and Stanier, R. Y. (1979) *J. Gen. Microbiol. 111*, 1−61.
33. Tang, X.-S., and Diner, B. A. (1994) *Biochemistry 33*, 4594−4603.
34. Tamura, N., and Cheniae, G. (1987) *Biochim. Biophys. Acta 890*, 179−194.
35. Lichtenthaler, H. K. (1987) *Methods Enzymol. 148*, 350−382.
36. Palaniappan, V., Aldema, M. A., Frank, H. A., and Bocian, D. F. (1992) *Biochemistry 31*, 11050−11058.
37. Palaniappan, V., Martin, P. C., Chynwat, V., Frank, H. A., and Bocian, D. F. (1993) *J. Am. Chem. Soc. 115*, 12035−12049.
38. Pakrasi, H. B., and Vermaas, W. F. J. (1992) in *The Photosystems: Structure, Function, and Molecular Biology* (Barber, J., Ed.) pp 231−257, Elsevier Science Publishers, Amsterdam.
39. Lutz, M., and Mantele, W. (1991) in *Chlorophylls* (Scheer, H., Ed.) pp 855−902, CRC Press, Boca Raton.
40. Tasumi, M., and Fujiwara, M. (1986) *J. Phys. Chem. 90*, 250−255.
41. Koulougliotis, D., Tang, X.-S., Diner, B. A., and Brudvig, G. W. (1995) *Biochemistry 34*, 2850−2856.
42. Rutherford, A. W., and Nitschke, W. (1996) in *Origin and Evolution of Biological Energy Conservation* (Baltscheffsky, H., Ed.) pp 143−175, VCH, New York.
43. Mac, M., Tang, X.-S., Diner, B. A., McCracken, J., and Babcock, G. T. (1996) *Biochemistry 35*, 13288−13293.
44. van Gorkom, H. J., and Schelvis, J. P. M. (1993) *Photosynth. Res. 38*, 297−301.